

Some Characteristics of Galactic Cepheids Relevant to the Calibration of the Distance Scale

Anwesh Mazumdar¹ and D. Narasimha²

Department of Astronomy and Astrophysics, Tata Institute of Fundamental Research,
Homi Bhabha Road, Mumbai 400005, India.

ABSTRACT

An analysis of the observed characteristics of the Galactic Cepheid variables is carried out in the framework of their period–luminosity relation being used as a standard candle for the distance measurement. The variation of the observed number density of Galactic Cepheids as function of their period and amplitude along with stellar pulsation characteristics is used to divide the population into two groups: one with low periods, probably multi-mode or higher mode oscillators, and another of high period variables which should be dominantly fundamental mode radial pulsators. Methods to obtain extinction-corrected colors from multi-wavelength observations of the second group of variables are described and templates of the $(V - I)$ light curves are obtained from the V light curves. Colors computed from the model atmospheres are compared with the extinction-corrected colors to determine the Cepheid instability strip in the *mean surface gravity–effective temperature diagram*, and relations are derived between mean colors $(B - V)$ vs *period of pulsation*, $(V - I)$ vs *period*, and $(V - I)$ at the *brightest phase vs amplitude of pulsation*. The strength of the κ -mechanism in the envelope models is used to estimate the metal dependency of the instability strip from which an idea of the sensitivity of the period–luminosity relation to the helium and metal abundance is given. Some estimate of the mass of Cepheids along the instability strip is provided.

Subject headings: Cepheids — dust, extinction — stars: oscillations — stars: statistics

¹e-mail: anwesh@astro.tifr.res.in

²e-mail: dna@astro.tifr.res.in

1. Introduction

The classical Cepheid variables provide an important standard candle to measure distances to galaxies up to ~ 30 Mpc. The Cepheid Distance Scale is considered to be among the most reliable methods because the physics of Cepheid pulsation is well-understood and the relation between the pulsation period and luminosity of the star is observationally well-established. The Cepheids are luminous, have a narrow range of surface temperatures; their pulsation is very stable and exhibit large amplitude. The intrinsic scatter in their period–luminosity relation is believed to be only around 0.3 mag. However, the Cepheid distance scale cannot be directly calibrated from the observation of nearby stars and consequently, several systematic effects still undermine its effectiveness as a standard primary candle to determine extragalactic distances beyond a few Mpc. Some of the questions which have direct bearing on the problem of distance calibration, but whose answers remain inconclusive in spite of extensive research, are listed below.

- Are the preferential pulsation modes of Cepheids period-dependent?
- Is a single period–luminosity relation applicable to the entire instability strip?
- Is the period–luminosity relation modified appreciably due to metallicity dependency of the stellar structure?
- Is the period–luminosity–color relation a better indicator of distance than the period–luminosity relation only?

Iben and Tuggle (1975) numerically computed the period and luminosity of Cepheids for a range of masses and obtained a relation between metallicity, surface temperature, period and luminosity. The period–luminosity–color relation is found to be dependent on metallicity due to extreme sensitivity of the color–temperature relation on chemical composition. However, according to Becker, Iben and Tuggle (1977), within the uncertainties, the relation between period and luminosity for the first and second crossings of the Cepheid instability strip by a particular star does not crucially depend on the chemical composition. Since the time spent in traversing the strip is largest for the second crossing, most of the observed Cepheids are in this stage of evolution. So, although conversion of the period into a V -magnitude will introduce small effects due to surface temperature and metallicity, a period–luminosity relation derived from observations should not be affected by small variations in the chemical composition. Indeed, the robustness of the period–luminosity relation against changes in the chemical composition is borne out by theoretical as well as observational studies. The theoretical models of Bressan et al. (1993) produce the same period (within

an error of 2%) for a given luminosity, irrespective of the chemical composition. From observations of Cepheids in M31, it appears that there is no significant dependence of the period–luminosity zero point on metallicity gradients (Freedman & Madore 1990). The recent review on the metallicity dependence of the Cepheid Distance Scale in the context of the HST Key Project on Extragalactic Distance Scale (Kennicutt et al. 1998) also leads to the same conclusion. Similarly, even though color-color diagram of Cepheids can be used to determine their metallicity, it is not an improvement in terms of its application to the estimation of distances, given that after extinction correction the color has larger error than the V -magnitude (e.g., Fouqué & Gieren 1993). Clearly, in order to address the above question, systematic work is required on the pulsation properties, evolution as well as stellar atmospheric structure, taking into account the onset of convection in the atmosphere during the pulsation cycle.

In the present study we shall adopt the working hypothesis that the luminosity of the star *as a function of period* is not directly altered by metallicity (subject to the star being a classical Cepheid), and that the color of the star provides a better diagnostic for the estimation of extinction than for the determination of the distance. We devise methods to determine the extinction by the interstellar medium, and particularly emphasize the importance of observations in multi-wavelength bands, and also address the question of pulsation modes of Cepheids.

The Cepheids in our own Milky Way galaxy have been observed by several astronomers over the years, and it is possible to obtain multi-wavelength data as well as accurate periods for a large number of them. A careful analysis of these Galactic Cepheids will naturally provide a useful template for identifying and estimating the various errors in the calibration of the Cepheid Distance Scale. A robust calibration of this distance scale is particularly important for extending it to extragalactic domains, as Cepheids are being observed in several far away galaxies, including those in the Virgo Cluster, by the Hubble Space Telescope. The hope is that distances based on these observations will ultimately lead to an accurate determination of the Hubble Constant. In this context, we attempt to provide a new calibration of the Cepheid Distance Scale, which is free from many of the systematic errors. In an accompanying communication (which we will refer to as Paper II), we apply these results for estimating the distance to the Virgo Cluster, based on the HST data for the Cepheids in the spiral M100.

This paper is organized as follows. In Section 2 we discuss the number distribution of Cepheids against their periods. In Section 3, we demonstrate the feasibility of obtaining accurate $(V - I)$ light curves from the V light curve of a Cepheid and limited number of observations in the I band. This method is particularly useful for analyzing Cepheid data with

few observations in one band (as in HST observations). In Section 4, we devise a formalism for extinction correction for each individual Cepheid, based on model atmospheres and an R_V -dependent extinction law. Several useful period–color and amplitude–color relationships are also derived. Section 5 is concerned about the different modes of pulsation of Cepheid variables and their manifestations in the observed properties like period and amplitude of pulsation. We argue that it is necessary to choose the correct lower cutoff period in the period–luminosity relation in order to prevent contamination from multi-mode pulsators. In Section 6, we give an estimate for Cepheid masses at different periods, based on our results about the instability strip in the surface gravity versus effective temperature plane. Some discussion on the metallicity effects are presented in Section 7 and the major limitations of the present work are listed in Section 8. The main conclusions from this work are summarized in Section 9.

2. Number Distribution of Galactic Cepheids

The classical Cepheid variables are radially pulsating giants and supergiants, having pulsation periods in the range of less than a day to upwards of 100 days. Their amplitude of light variation in the V (Johnson) band may be up to nearly 2 magnitudes although most of the Cepheids have amplitude between 0.6 to 1.3 magnitude. The General Catalogue of Variable Stars (GCVS) (Kholopov et al. 1988) provides a nearly exhaustive list of all the Cepheids observed in the Milky Way Galaxy along with their periods and V amplitudes. Our principal source of photometric data for the Galactic Cepheids was in the electronic form from the McMaster Cepheid Photometry and Radial Velocity Data Archive, which contains detailed Julian Day versus magnitude data in multiple wavelengths from different observers. Among the various sources available at this website, we have chosen to use data mainly from Coulson & Caldwell (1985), Coulson, Caldwell & Gieren (1985), and in some cases from Berdnikov (1992), and Berdnikov & Turner (1995). The former two sources were preferred because they provided homogeneous data in UBV (Johnson) and I (Cousins) passbands. The latter sources were used to supplement data in U, B and I bands. However, our choice of stars is severely limited because we require data in all these four filters without internal inconsistencies in order to carry out extinction correction.

From the GCVS, a distribution of nearly all classical Cepheids in the Galaxy, over a period range of 2 to 65 days is obtained. We have displayed the moving averaged number density of Cepheids against the logarithm of their periods in days ($\log(P)$) in Figure 1. It is evident that the majority of Cepheids observed in our galaxy have periods less than 10 days. There is a small dip in the number density around a period of 8–15 days. We fit a Gaussian

curve to the number distribution pattern at low periods, and find that the distribution function may be split into two components. Below a period of 8 days, many of the Cepheids are multi-mode pulsators, in which the fundamental mode may not be the dominant one. These Cepheids occupy the main peak in Figure 1. Above period of around 15 days, nearly all the Cepheids are single mode pulsators. (The issue of modes of pulsation is discussed in detail in Section 5). In the intermediate range of periods, there exists a transition zone where not many Cepheids are observed.

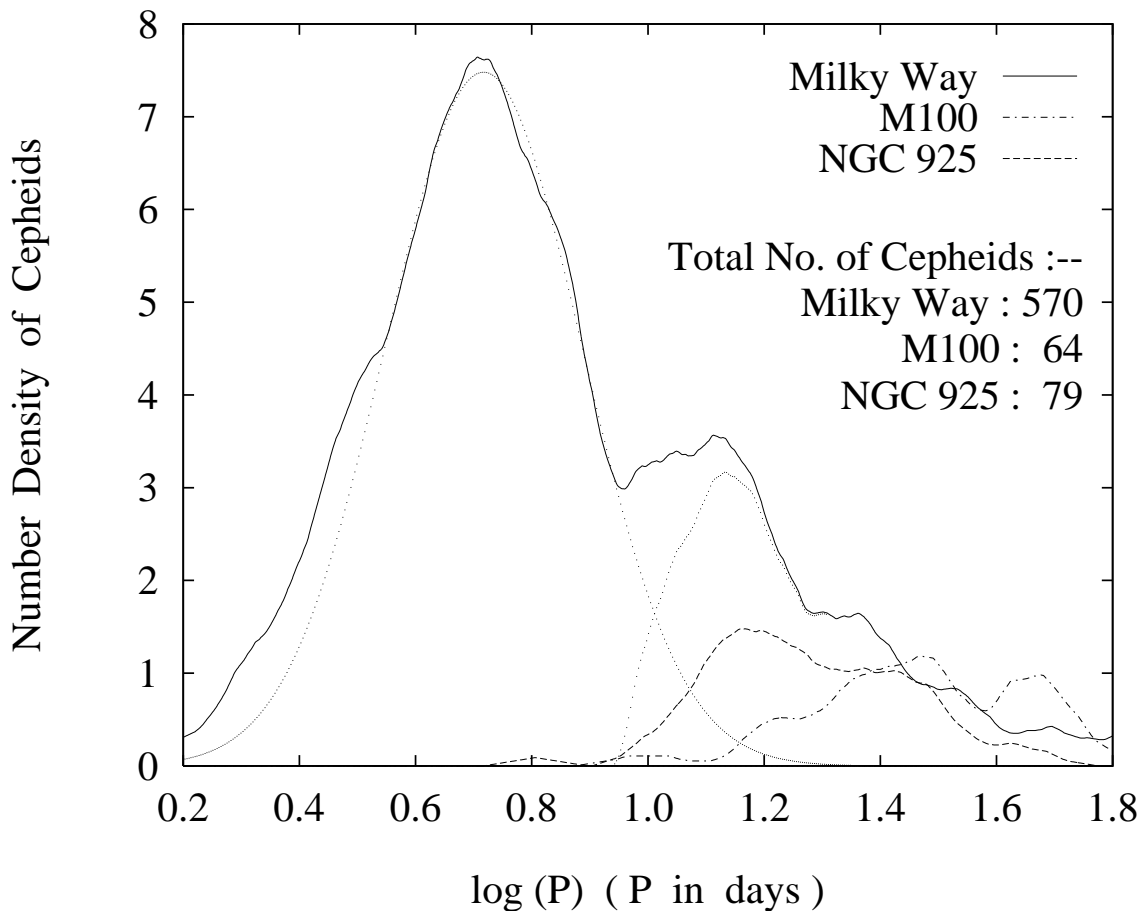


Fig. 1.— The number density distribution against $\log(P)$ is shown for Cepheids in the Milky Way, as well as in two other galaxies (observed by HST). A moving average has been used to generate a smooth curve from discrete observations. The Galactic sample can be split up into two populations (shown by the dotted lines), having slight overlap between periods of 9 and 18 days.

We also studied the number density distribution of Cepheids in some of the galaxies

being observed by HST. Two examples (M100 and NGC 925) (Ferrarese et al. 1996; Silbermann et al. 1996) are plotted along with the Milky Way distribution in Figure 1. We believe that in these galaxies, probably due to flux limitation, only the higher period Cepheids have been detected. These pulsators follow the same number density pattern as shown by Galactic Cepheid variables. Thus, for the analysis of these extragalactic Cepheids, the template should be built on Galactic Cepheids having period $\log(P) \geq 1.15$ only, and low period overtone Cepheids should be avoided. The implications of this preferred selection on the slope of the period–luminosity relation will be discussed in Paper II.

3. Synthetic Light Curves

For extragalactic Cepheids, usually the V (Johnson) band observations have good phase sampling, from which generally it is possible to construct a reliable light curve. However, for observations in other filters, though equivalent of the I (Cousins) band is a popular choice, often the phase coverage is not good, and it is difficult to obtain a light curve with correct values for the various parameters like amplitude or peak and mean brightness. For Galactic Cepheids, however, in many cases the data is well-sampled for all the bands, and it is possible to obtain reliable light curves for the multi-wavelength bands and the colors as well. It is instructive as well as useful to compare the general shapes of light curves of different colors like $(B - V)$, $(V - I)$ with that of the V light curve of a particular Galactic Cepheid. We attempt to produce a reasonably accurate light curve for the $(V - I)$ color from the V light curve of a given Cepheid. Although such attempts to obtain light curves in other bands from V light curve have been made before (e.g., Labhardt, Sandage & Tammann 1997), our approach is based on the phase difference between the flux variability and the color variability and is primarily intended to estimate mean $(V - I)$ and its peak value when the I band phase coverage is poor.

We find that the V and the $(V - I)$ light curves of the galactic Cepheids are very similar, except for a small phase difference between the maximum and minimum and the shape of the curves in the descending branch (i.e., in the part from the minimum magnitude to the maximum). Consequently, it is possible to simulate the $(V - I)$ light curve from the V light curve in the following way. We first reduce the V light curve to a normalized version, having magnitude of ± 1 at minimum and maximum, and phase running from -0.5 to $+0.5$, with the phase of the maximum brightness (defined as V_{\max} , having the minimum magnitude value) being taken as the zero point. The phases ϕ_{\max} and ϕ_{\min} correspond to the phases where the V -magnitude value is minimum and maximum (i.e., brightest and dimmest) respectively.

We define

$$\begin{aligned}
 V_{\max} &= V(\phi_{\max}) \\
 V_{\min} &= V(\phi_{\min}) \\
 \phi' &= \phi - \phi_{\max} \\
 \phi_0 &= \phi_{\min} - \phi_{\max} \\
 \phi_n &= \begin{cases} \phi' + 1, & \text{if } \phi' \leq 0.5 \\ \phi' - 1, & \text{if } \phi' > 0.5 \\ \phi', & \text{otherwise} \end{cases} \\
 \overline{V} &= \frac{V_{\min} + V_{\max}}{2} \\
 \Delta V &= V_{\min} - V_{\max} \\
 V_n(\phi_n) &= \frac{V(\phi) - \overline{V}}{\Delta V}
 \end{aligned} \tag{1}$$

It should be noted that the quantity \overline{V} is only the average of the V maximum and minimum magnitudes, and should not be confused with the flux-averaged mean V magnitude, for which we reserve the symbol $\langle V \rangle$. We note that the following transformation produces a light curve which is very nearly identical to the $(V - I)$ light curve.

$$(V - I)_{\text{synth}}(\phi_n) = \begin{cases} V_n(\phi_n \cdot \frac{\phi_0}{\phi_0 - 0.04}) & \text{if } -0.5 \leq \phi_n < 0 \\ V_n(\phi_n \cdot \frac{\phi_0 - 0.07}{\phi_0}) & \text{if } 0 \leq \phi_n \leq +0.5 \end{cases} \tag{2}$$

We can reconstruct the $(V - I)$ light curve in the correct units of magnitudes from this $(V - I)_{\text{synth}}$ by making the inverse transformation of equation (1) as follows:

$$(V - I)(\phi_n) = \overline{(V - I)} + \Delta(V - I) \cdot (V - I)_{\text{synth}}(\phi_n) \tag{3}$$

where

$$\begin{aligned}
 \overline{(V - I)} &= \frac{(V - I)_{\min} + (V - I)_{\max}}{2} \\
 \Delta(V - I) &= (V - I)_{\min} - (V - I)_{\max}
 \end{aligned}$$

Note once again that this average $\overline{(V - I)}$ is different from the flux-averaged $\langle V - I \rangle$. The actual light curves and the synthesized light curve for one Cepheid are shown in Figure 2 for comparison. Although the synthetic light curve does not match the actual light curve exactly at all phases, it is good enough to obtain the value of the mean magnitude, $\langle V - I \rangle$, and the amplitude, $\Delta(V - I)$, within errors of 0.01 mag.

However, we should stress that all the following analysis for the Galactic Cepheids was based on the *actual* V and $(V - I)$ light curves, and not on the *synthetic* light curves described

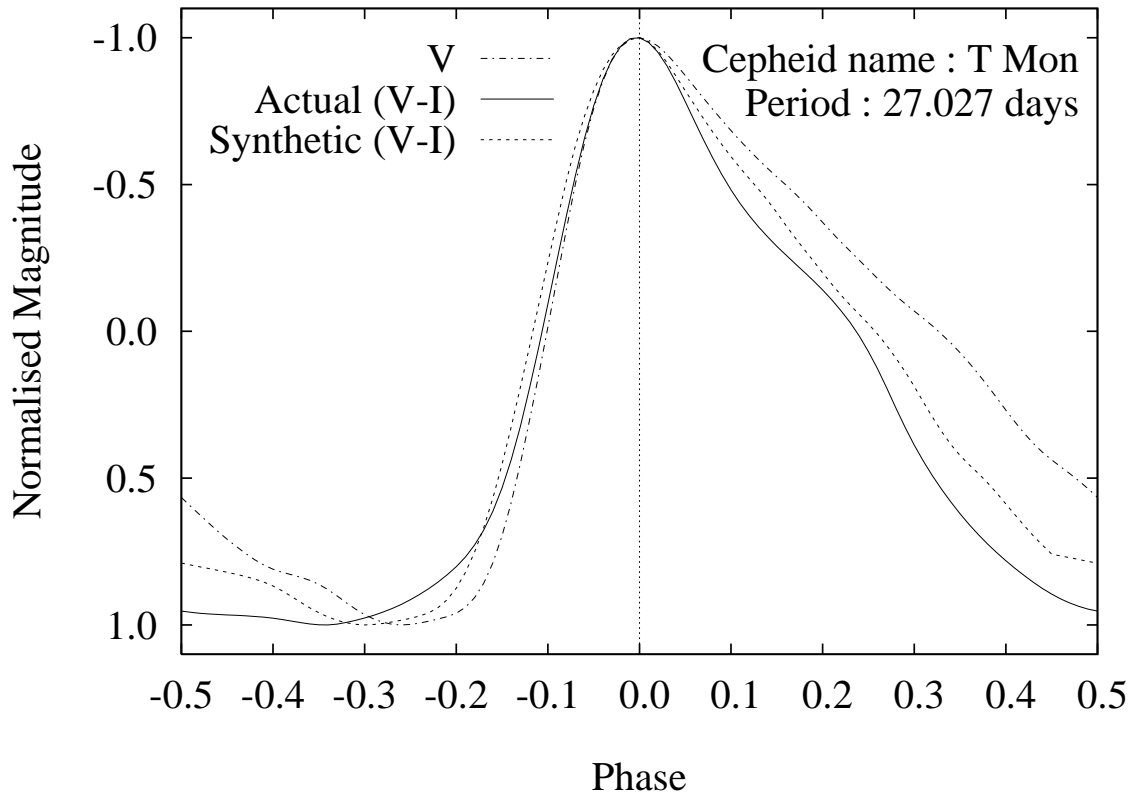


Fig. 2.— Typical light curves of a Galactic Cepheid are shown. The $(V - I)$ light curve is seen to follow the V light curve with a small phase difference. By adjusting this phase difference, a synthetic light curve for $(V - I)$ may be generated from the V light curve, which closely simulates the actual $(V - I)$ light curve.

above. This exercise of synthesizing the $(V - I)$ light curve from the V light curve was carried out in order to prepare and to scrutinize a template for obtaining reasonably accurate light curves and the associated quantities like amplitude, mean and peak brightness for data sets where observations in I band are inadequate to produce independent light curves for $(V - I)$. This method later proved to be extremely useful for estimating the reddening in the HST data for Cepheids, which we shall discuss in Paper II.

4. Extinction Correction

The Galactic Cepheid variables have generally large extinction (typically more than 1 mag). The extinction renders the raw colors as well as the V -magnitude useless even

if we know the distance to a Cepheid. However, considerable work has been carried out to correct for extinction by studying the spectral characteristics of a background hot star, which are modified due to absorption in the interstellar medium. In the present work, we have carried out the extinction correction for the Galactic Cepheids by the following formalism. According to Cardelli, Clayton & Mathis (1989), in grain-dominated interstellar medium, the extinction law can be parameterized by the quantity R_V ($= A_V/E(B - V)$). Based on this R_V -dependent extinction law for different wavelengths, we found that it is possible to derive a extinction-free quantity in terms of the standard broadband filter colors. The mean extinction-dependence is of the form

$$A_\lambda/A_V = a(\lambda) + b(\lambda)/R_V, \quad (4)$$

where $a(\lambda)$ and $b(\lambda)$ are given polynomials in λ^{-1} , for $1.1 \mu\text{m}^{-1} \leq \lambda^{-1} \leq 3.3 \mu\text{m}^{-1}$. From this, the following relations for the reddenings can be derived.

$$\begin{pmatrix} E(U - B) \\ E(B - V) \\ E(V - I) \end{pmatrix} = \begin{pmatrix} a(U) - a(B) & b(U) - b(B) \\ a(B) - a(V) & b(B) - b(V) \\ a(V) - a(I) & b(V) - b(I) \end{pmatrix} \begin{pmatrix} A_V \\ A_V/R_V \end{pmatrix} \quad (5)$$

For the standard Johnson-Cousins UBVI filters, the coefficients $a(\lambda)$ and $b(\lambda)$ are given by,

$$\begin{aligned} a(U) &= 0.95346 & b(U) &= 1.90555 \\ a(B) &= 0.99975 & b(B) &= 1.00680 \\ a(V) &= 1.00000 & b(V) &= 0.00000 \\ a(I) &= 0.78421 & b(I) &= -0.56543 \end{aligned}$$

From Equation 5, we may write

$$\begin{pmatrix} E(U - B) \\ E(B - V) \\ E(V - I) \end{pmatrix} = \begin{pmatrix} -0.04629 & 0.89875 \\ -0.00025 & 1.00680 \\ 0.21579 & 0.56543 \end{pmatrix} \begin{pmatrix} A_V \\ A_V/R_V \end{pmatrix} \quad (6)$$

As may be seen from above, the coefficient $a(B) - a(V)$ is a very small quantity, and we may approximately equate it to zero. Hence we define an extinction-independent quantity Q as

$$\begin{aligned} Q &\simeq -[(U - B)_0 - (B - V)_0] - 0.21 [(V - I)_0 - (B - V)_0] - 0.20 (B - V)_0 \\ &= -[(U - B) - (B - V)] - 0.21 [(V - I) - (B - V)] - 0.20 (B - V) \end{aligned} \quad (7)$$

The stellar atmospheric structure is determined from the value of the surface gravity, g , the effective temperature, T_{eff} and the chemical composition (subject to the uncertainties due

to mechanical energy transport and dissipation in the atmosphere). The Cepheid instability strip on the HR diagram can be mapped on to a similar strip in the $\log T_{\text{eff}} - \log g$ plane. We determine the position of the strip in the $\log T_{\text{eff}} - \log g$ plane from observations and model atmospheres as follows. We use synthetic colors computed by Bessell, Castelli, & Plez (1998) based on the latest Kurucz model atmospheres to obtain theoretical plots of $(U - B)_0$ and $(V - I)_0$ against $(B - V)_0$ for classical Cepheids within the period range of 15 to 60 days for an assumed $\log T_{\text{eff}} - \log g$ relation. In this way, a theoretical plot of Q as a function of $(B - V)_0$ is produced. By demanding that Q be independent of extinction for each Cepheid, we can find out the amount of reddening $E(B - V)$ from this plot, if the Cepheids were to occupy a line in HR diagram. But due to the errors in observations as well as the finite width of the instability strip, we use the Q diagram together with the $(B - V)_0$ vs $\log(P)$ relation to determine the reddening correction.

Since the Cepheid instability occurs within a narrow range of temperature in the HR diagram, for a limited range of $\log(P)$ it is reasonable to deduce the existence of a linear relationship between $\langle B - V \rangle_0$ (which is a measure of T_{eff}) and $\log(P)$ (which is related to the luminosity through the period–luminosity relation). Indeed, such a relation has been found to hold true earlier also (e.g. Feast & Walker 1987), albeit with a different slope compared to what we obtain. We have used a relation of the form

$$\langle B - V \rangle_0 = a \log P + b,$$

with unknown coefficients a and b . On minimizing the total χ^2 deviation of this relation, along with the Q vs $\langle B - V \rangle_0$ graph (Figure 3), we obtain the reddening $E(B - V)$.

After the extinction correction is carried out, we can compare the $(U - B)_0$ and $(V - I)_0$ for a Cepheid having a specified $(B - V)_0$ with the corresponding theoretical values obtained from model atmospheres for the assumed strip in the $\log T_{\text{eff}} - \log g$ plane (Figure 4). By varying the slope and intercept of the strip, we can determine the theoretical position of the Cepheids in the $\log T_{\text{eff}} - \log g$ plane by demanding that the $(U - B)_0$ vs $(B - V)_0$ and $(V - I)_0$ vs $(B - V)_0$ computed from model atmospheres should individually match the corresponding values derived from the Q diagram. The strip in the $\log T_{\text{eff}} - \log g$ plane which gives the best agreement with the observed colors after reddening corrections is shown in Figure 5.

Though we started with a fairly large sample, only 25 of the Cepheids with $\log(P) \geq 1.15$ had observations in U, B, V and I bands, showing tolerable consistency among different observers. Their periods and photometric magnitudes (which we obtained by integrating the light curves) are listed in Table 1. One of the Cepheids, KQ Sco, had very large reddening ($E(B - V) > 1$ mag), and since one is not sure about the applicability of our statistical formalism to such cases, we chose not to include it in our sample.

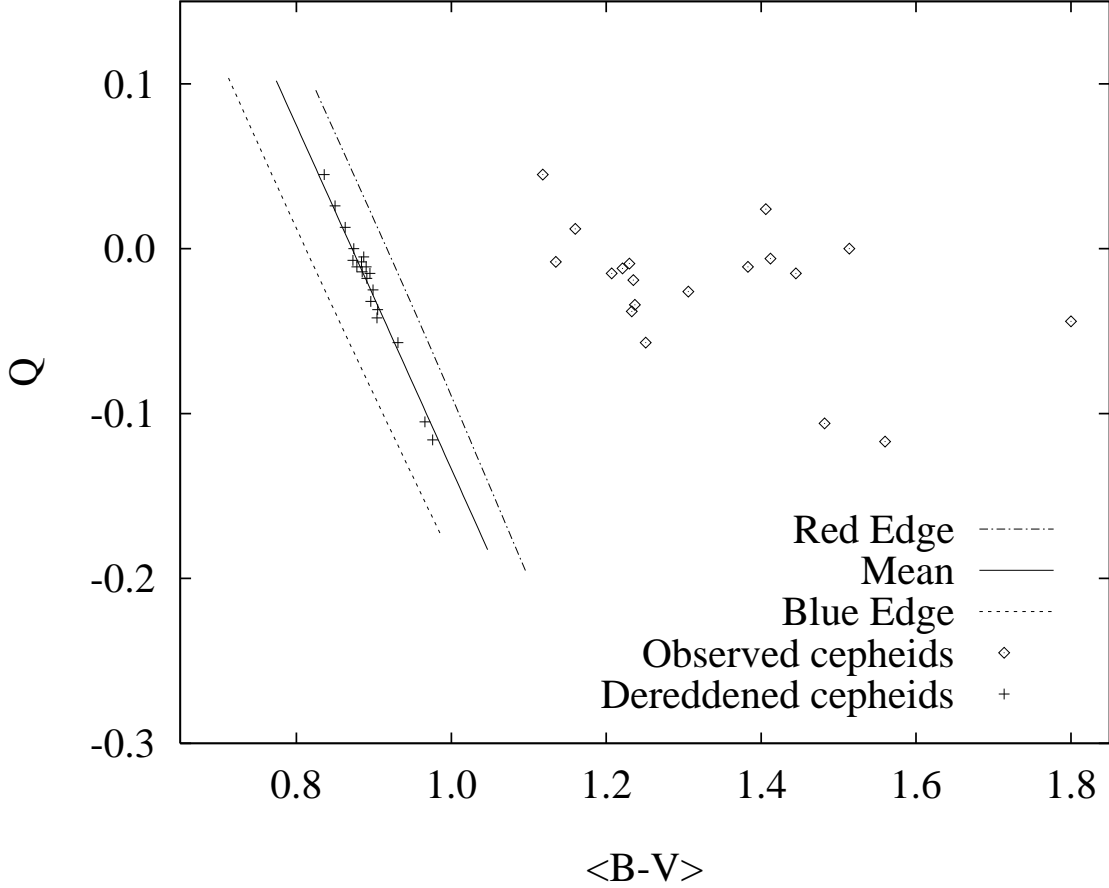


Fig. 3.— The Q Diagram: The extinction-independent quantity Q is plotted against $\langle B - V \rangle$ for the red edge, the blue edge and the mean of the Cepheid Instability Strip. The lines are drawn from the model stellar atmospheres on a strip on the $\log T_{\text{eff}} - \log g$ plane. The observed Galactic Cepheids (Table 1) whose $\langle B - V \rangle$ are increased due to reddening, should actually occupy positions within this strip (indicated by “+”) after dereddening.

We based the selection of the $\log T_{\text{eff}} - \log g$ strip on two criteria: (1) the regained positions of the Cepheids on the $\log T_{\text{eff}} - \log g$ plane should conform to the original assumed strip; (2) theoretical constraint—using the period–luminosity relation (Paper II), we can obtain the period of a star as a function of g and T_{eff} :

$$0.65 \log(P) = -0.5 \log g - \log T_{\text{eff}} + \log Q_0, \quad (8)$$

where Q_0 is a quantity depending on the effective polytropic index, which decreases slowly from around 0.025 to 0.015 when the period increases from 15 to 60 days. Considering the

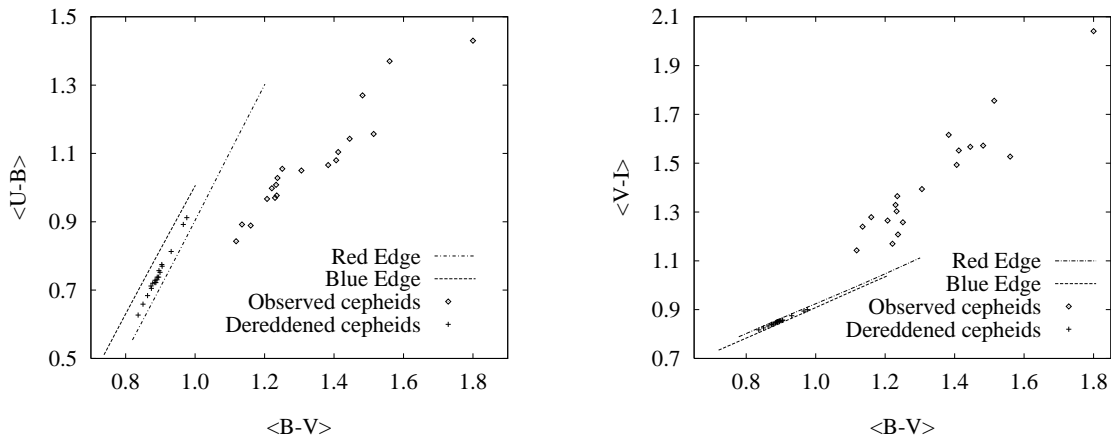


Fig. 4.— The color–color diagrams for the Cepheid instability strip are shown. The positions of 19 Galactic Cepheids, before and after reddening correction, are also shown.

narrow T_{eff} range of the instability strip, the magnitude of the slope of $\log g$ against $\log(P)$ should not exceed 1.35. For our present analysis, we allow the permissible value of the the slope to be in the range 1.2 to 1.35. We find that at higher T_{eff} values the upper limit of the slope of $\log g$ against $\log(P)$ is exceeded, even for a low inclination of the assumed initial strip. Further, at higher inclinations, the regained T_{eff} and g values are completely at variance with the assumed strip (Figure 6). On the other hand, at low T_{eff} for medium to high inclinations of the strip, although the first condition is satisfied, the slope of $\log g$ against $\log(P)$ is far too low. If we decrease the inclination at low T_{eff} the regained positions of the Cepheids do not match the original strip (see Figure 6). At intermediate temperatures, the limits on the inclination of the strip are determined by using both the conditions.

This is the way we converge to the strip shown in Figure 5. The slope of the $\log g$ vs $\log(P)$ graph for the accepted strip turns out to be -1.26 (Figure 7), which is in agreement with the constraint obtained on theoretical grounds. Two typical discrepant strips are shown in Figure 6 for comparison. It should be noted that the narrow scatter of the points around the mean line on the $\log T_{\text{eff}} - \log g$ plane is an artifact of the statistical methods used here. Since we have used only two constraints (namely, the $\langle B - V \rangle_0$ vs $\log(P)$ relationship and the Q diagram), the minimization procedure causes the points to be clustered in the final diagrams. The intrinsic width of the instability strip is not borne out by our converged strip, but the mean position of the stars should be considered to be acceptable for Cepheids in their core helium burning phase. It turns out that five among the 24 Cepheids we selected (*viz.*, XZ Car, CD Cyg, SZ Aql, WZ Sgr and KN Cen) consistently fall at far too low or high g after the minimization. We interpret it as an indication that these stars might be in

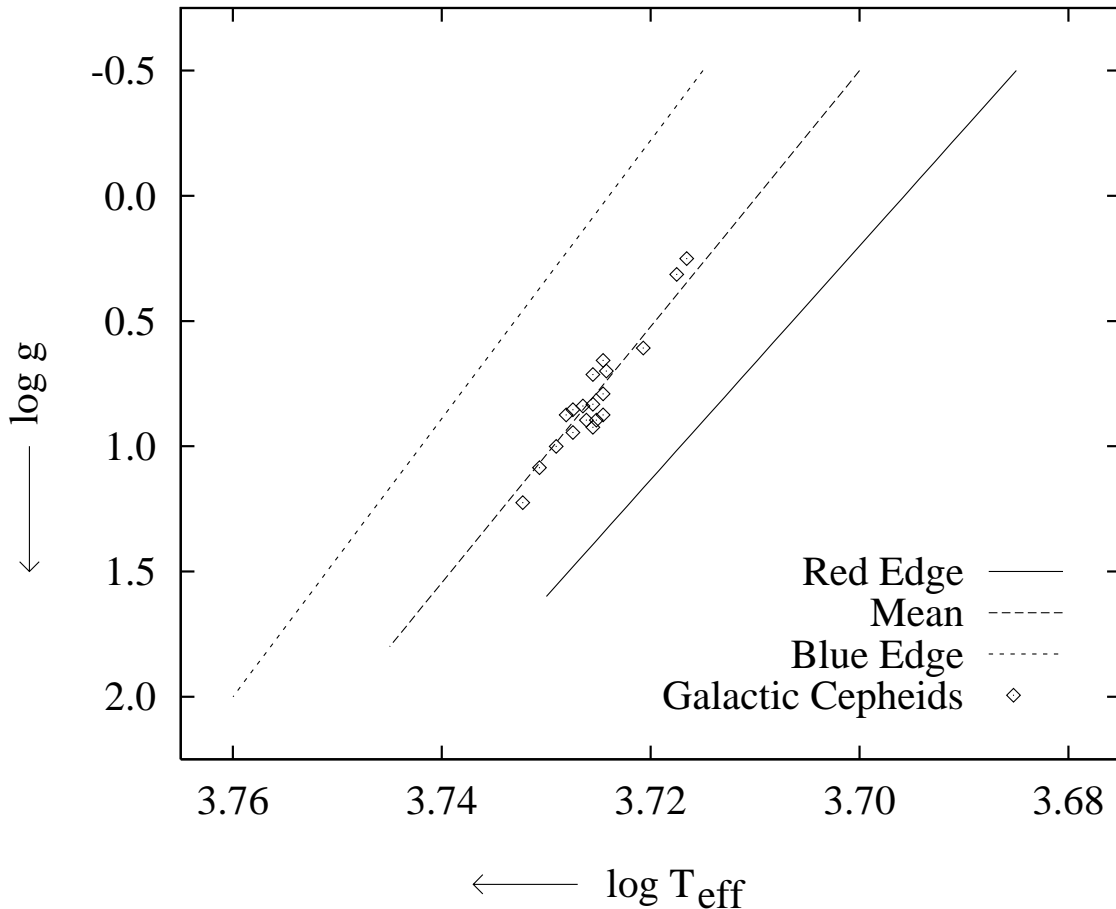


Fig. 5.— The Cepheid instability strip is plotted on the $\log T_{\text{eff}} - \log g$ plane. The positions of 19 Galactic Cepheids, derived from their dereddened colors, are also shown.

their first or third passage of the instability strip rather than in the slow blue-ward passage during core helium burning. Consequently, these five stars were not included in our final analysis. Independently such a conclusion was arrived at by Gieren (1989) for some of these stars, but in two instances (*viz.*, VY Car and AQ Pup) our results are different.

We obtained a similar strip by combining the evolutionary tracks of Bressan et al. (1993) and the luminosity and temperature values given for the two edges by Chiosi, Wood and Capitanio (1993). On comparison between this strip and that shown in Figure 5, we find that our values of the surface gravity are lower at the high period end than that of Bressan et al. and Chiosi et al. This implies that we have a higher luminosity at the high period

Table 1: Periods and photometric parameters of Galactic Cepheids

Name	P (days)	V	$(U - B)$	$(B - V)$	$(V - I)$
VW Cen	15.036	10.231	1.080	1.406	1.493
SV Mon	15.234	8.260	0.843	1.118	1.143
XX Car	15.711	9.325	0.892	1.135	1.240
XZ Car	16.651	8.596	1.102	1.317	1.379
CD Cyg	17.071	8.980	1.220	1.430	1.492
Y Oph	17.127	6.124	1.066	1.383	1.616
SZ Aql	17.138	8.650	1.340	1.540	1.601
YZ Car	18.165	8.714	0.889	1.160	1.279
VY Car	18.912	7.482	1.028	1.237	1.208
RU Sct	19.698	9.480	1.430	1.800	2.041
RY Sco	20.317	8.018	1.157	1.514	1.756
RZ Vel	20.397	7.079	0.967	1.207	1.265
WZ Sgr	21.850	8.030	1.302	1.476	1.521
WZ Car	23.015	9.274	0.970	1.230	1.329
VZ Pup	23.172	9.626	0.977	1.235	1.365
SW Vel	23.441	8.119	1.008	1.233	1.303
X Pup	25.965	8.513	1.050	1.306	1.394
T Mon	27.027	6.131	0.998	1.221	1.170
RY Vel	28.140	8.360	1.104	1.412	1.552
KQ Sco	28.692	9.814	1.866	1.984	2.168
AQ Pup	30.072	8.681	1.143	1.445	1.567
KN Cen	34.023	9.856	1.130	1.657	1.882
U Car	38.807	6.293	1.055	1.251	1.258
RS Pup	41.660	6.996	1.307	1.482	1.572
SV Vul	45.103	7.240	1.370	1.560	1.527

end of the strip, which is vindicated by the higher slope of the period–luminosity relation, which we shall discuss in Paper II. The strip obtained from Bressan et al. and Chiosi et al. runs into inconsistencies for the reddening correction technique applied in the present work for Galactic Cepheids using model atmospheres (Bessell et al. 1998) when we compare the color–color diagrams $(U - B)_0$ vs $(B - V)_0$ and $(V - I)_0$ vs $(B - V)_0$ for the instability strip with those for the unreddened data.

For the converged instability strip in the $\log T_{\text{eff}} - \log g$ plane, the reddening $E(B - V)$ is obtained from the χ^2 minimization discussed earlier and the other reddenings $E(U - B)$

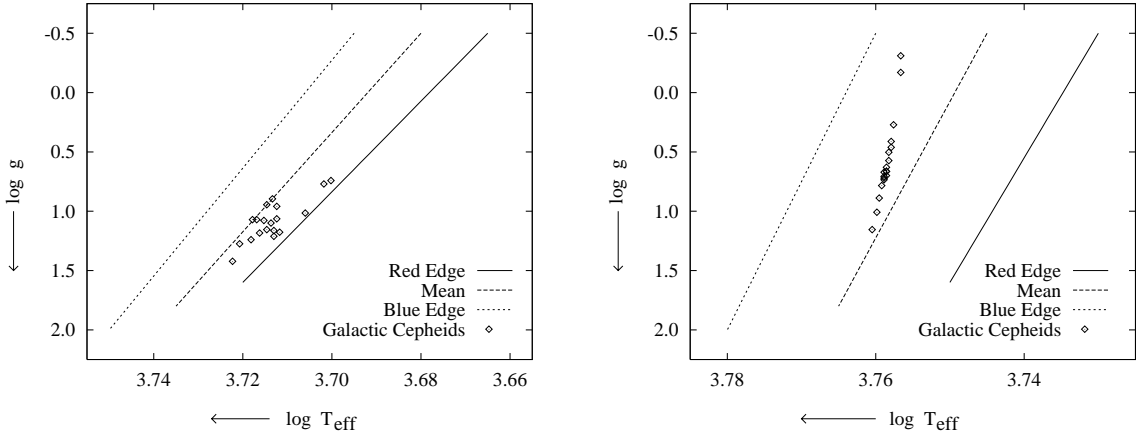


Fig. 6.— The Cepheid instability strip along with the derived positions of individual stars is plotted on the $\log T_{\text{eff}} - \log g$ plane, for two different choices of T_{eff} vs $\log g$: (a) Low T_{eff} and low value of $d \log g / d \log T_{\text{eff}}$, and (b) High T_{eff} and high value of $d \log g / d \log T_{\text{eff}}$. These lines provide a limit on the position of the red and blue edge of the strip.

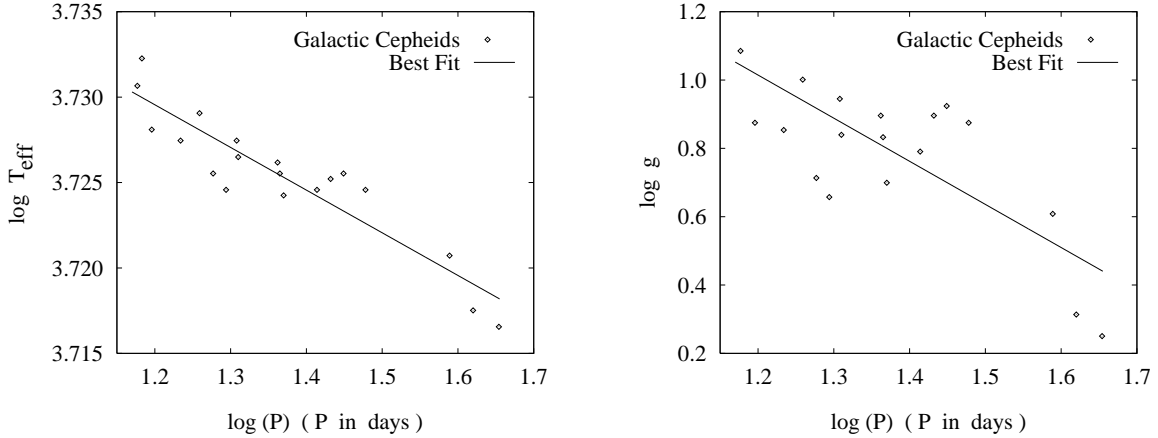


Fig. 7.— Logarithms of the effective temperature, T_{eff} , and the surface gravity, g , are plotted against $\log(P)$ for 19 Galactic Cepheids. The best fit linear relations are also shown.

and $E(V - I)$ are obtained from the color-color diagrams.

The reddening-corrected values $\langle U - B \rangle_0$, $\langle B - V \rangle_0$, $\langle V - I \rangle_0$ and $(V - I)_0|_{\text{at } V_{\text{max}}}$ are obtained for each Cepheid. We plot in Figures 8 and 9 the two quantities $\langle B - V \rangle_0$ and $\langle V - I \rangle_0$ against $\log(P)$ along with the corresponding best fit straight lines given by the

following relations.

$$\langle B - V \rangle_0 = 0.21 \log(P) + 0.60 \quad (9a)$$

$$(\chi^2 \text{ per degree of freedom}) = 0.016$$

$$\langle V - I \rangle_0 = 0.13 \log(P) + 0.67 \quad (9b)$$

$$(\chi^2 \text{ per degree of freedom}) = 0.008$$

We compare our derived reddenings with the values found in the literature, obtained by other methods (Table 2). We also compared the obtained $\langle B - V \rangle_0$ as a function of $\log(P)$ with similar relations given by others. Although the value of the slope of this linear relation is generally quoted to be around 0.4 (Fernie 1990; Feast & Catchpole 1997), we verified that between the period range of $1.15 \leq \log(P) \leq 1.65$, the slope is indeed 0.22 if we use the data from Fernie (1990), which is close to our derived value. The high value of the slope reported in the literature is valid only if low period Cepheids are considered or the unusually large $\langle B - V \rangle_0$ of one or two variables which we found to be at a different stage of evolution are included in the regression. This is an example of the differences in various Cepheid relations for high and low period ranges (see Section 5).

We also found that the color $(V - I)_0$ at the brightest phase of the Cepheid, i.e., $(V - I)_0|_{\text{at } V_{\text{max}}}$, bears a linear relationship with the amplitude of light variation, ΔV (Figure 9). (However, due to lack of sufficient data, this relationship could not be investigated for all the 19 Cepheids.) The derived relation is

$$(V - I)_0|_{\text{at } V_{\text{max}}} = -0.28\Delta V + 0.87 \quad (9c)$$

$$(\chi^2 \text{ per degree of freedom}) = 0.018$$

These latter two relations have been used later for extinction correction of the HST data on M100 (discussed in Paper II). Since the statistics of these relations are constrained by lack of sufficient data, these relations should be treated as indicative, and allowance has to be made for some uncertainty in the values of the coefficients. Also, since this analysis was restricted to the Galactic classical Cepheid variables only, the relations we have derived should be considered to be applicable to populations having chemical composition similar to the average over the Galactic distribution. Nevertheless, we are able to establish the existence of such linear relationships, and their usefulness for estimating dereddened colors will be illustrated in Paper II.

We tried the synthetic colors obtained from model atmospheres by various workers, but each appears to have some or other problem while comparing with observed values of

Table 2: Comparison of Reddenings of 19 Galactic Cepheids

Name	$\langle B - V \rangle_0$	$E(B - V)$			
		This work	Fernie ^a	DDO ^b	Caldwell ^c
VW Cen	0.850	0.556	0.523	0.448	0.418
SV Mon	0.836	0.282	0.300	0.249	0.229
XX Car	0.873	0.262	0.300	0.349	0.362
Y Oph	0.878	0.505	0.476	0.655	0.630
YZ Car	0.863	0.297	0.430	0.396	0.398
VY Car	0.896	0.341	0.390	0.243	0.230
RU Sct	0.904	0.896	0.820	0.957	0.965
RY Sco	0.874	0.640	0.730	0.777	0.702
RZ Vel	0.885	0.322	0.300	0.335	0.296
WZ Car	0.884	0.346	0.330	0.384	0.384
VZ Pup	0.891	0.344	0.350	0.471	0.478
SW Vel	0.905	0.328	0.340	0.349	0.356
X Pup	0.899	0.407	0.410	0.443	0.417
T Mon	0.890	0.331	0.370	0.209	0.172
RY Vel	0.887	0.525	0.240	0.562	0.558
AQ Pup	0.895	0.550	0.600	0.512	0.555
U Car	0.931	0.320	0.350	0.283	0.277
RS Pup	0.966	0.516	0.640	0.446	0.484
SV Vul	0.976	0.584	0.580	0.570	0.431

^aFrom Fernie & Hube (1968)

^bFrom the David Dunlap Observatory Database of Galactic Classical Cepheids (Fernie et al. 1995)

^cFrom Caldwell and Coulson (1987)

standard stars in the luminosity class and spectral type of our interest. Finally we selected the latest available tables from Bessell et al. (1998), but even there they suggested that they had to rescale their $(U - B)$ colors to agree with the observed colors of stars. As discussed later in Section 8, we found that their unscaled $(U - B)$ colors fit the Cepheids better, and it is desirable to increase it by 4%. It is thus evident that the present model atmospheric colors are not accurate enough for detailed extinction correction if we have to use the $(U - B)$ color. Our expressions involving only $\langle V - I \rangle_0$ and $(V - I)_{0|at V_{max}}$ circumvent this problem to some extent. But to test the sensitivity of our results to systematic error in the synthetic $(U - B)$ color, we have repeated our analysis with the model value of $(U - B)$ increased

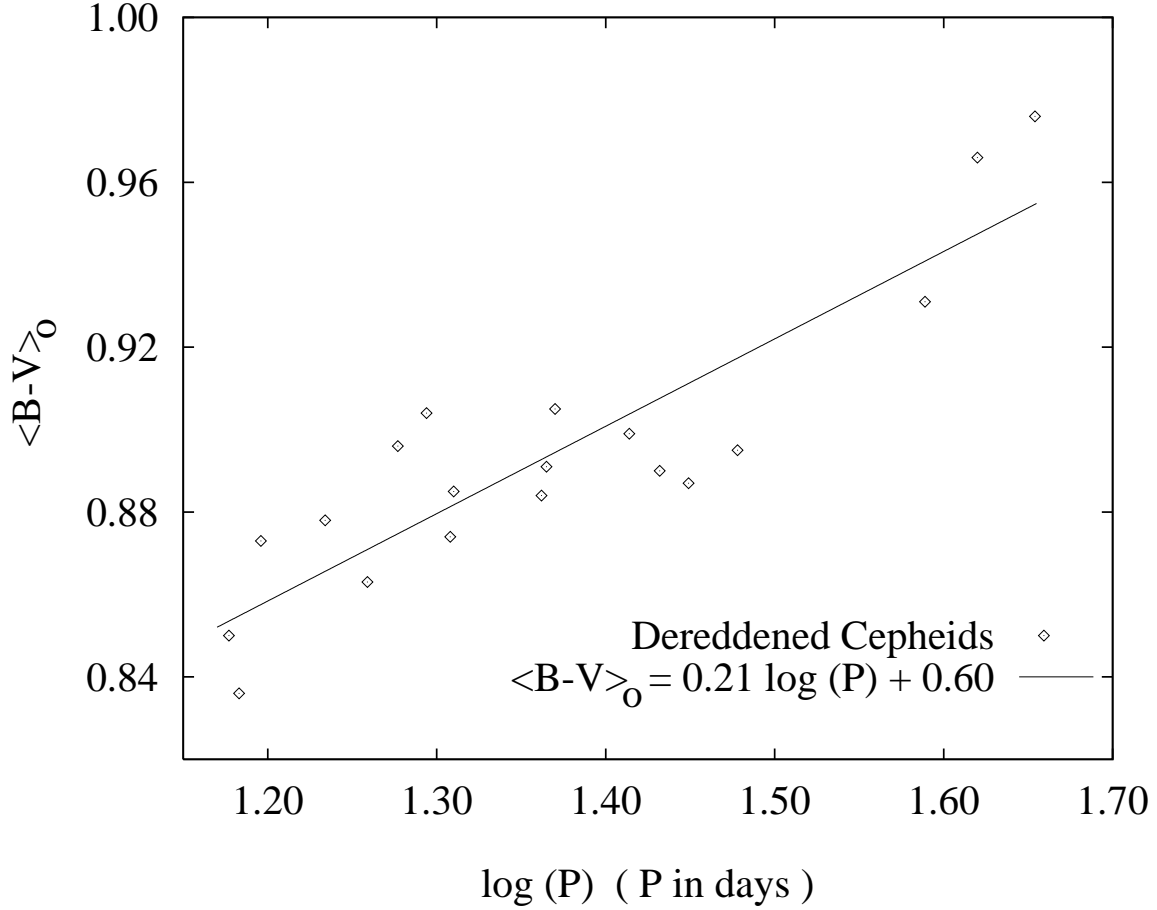


Fig. 8.— The dereddened color $\langle B - V \rangle_0$ is plotted against $\log(P)$ for 19 Galactic Cepheids. The best fit line, obtained from χ^2 minimization of this graph along with the Q diagram, is also shown.

by 1% for all g and T_{eff} values. Though the range of g at which the Cepheid variables of period between 15 and 60 days occupy changes by merely 20%, the converged expressions for period–color–amplitude relations do not show any appreciable change. For instance the three relations now become

$$\langle B - V \rangle_0 = 0.21 \log(P) + 0.62 \quad (10a)$$

$$\langle V - I \rangle_0 = 0.13 \log(P) + 0.69 \quad (10b)$$

$$(V - I)_0|_{\text{at } V_{\text{max}}} = -0.28 \Delta V + 0.88 \quad (10c)$$

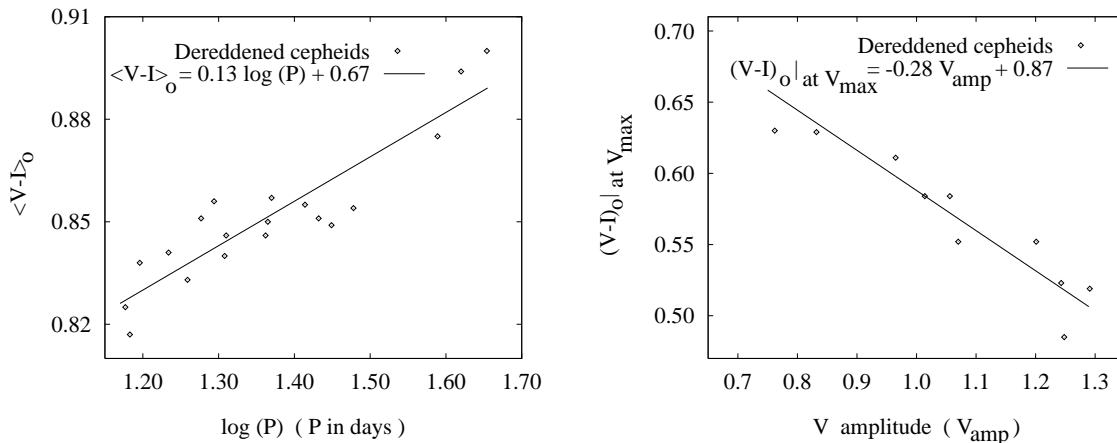


Fig. 9.— The color–period and color–amplitude relations are shown for Galactic Cepheids.

This indicates that the value of $(B - V)$ or $(V - I)$ after extinction correction at typical period of 30 days and 1 mag amplitude remains the same within 0.1%, provided that we use the same table of model atmospheres for our calibration of local Cepheids and extinction correction of extragalactic Cepheids at same range of periods.

5. Modes of Pulsation in Cepheids

Stars of zero-age-main-sequence mass in the range of $7M_{\odot}$ to $20 M_{\odot}$ traverse the Cepheid instability strip in the HR diagram thrice; first, red-wards during the contraction of the helium core, next blue-wards during core helium burning, and finally again red-wards during the shell-burning phase. The mass, luminosity as well as the effective polytropic index of the star will be different for the three phases and consequently, the period–luminosity relation is liable to vary slightly depending on the evolutionary phase. However, the duration of time over which a star traverses the instability strip is largest for the core helium burning stage (cf. Becker, Iben & Tuggle 1977) and we should probably expect approximately 90% of the Cepheids to be in this stage of evolution. From an inspection of the evolutionary models it turns out that for stars having constant surface temperature, the ratio of the central density to the mean density increases rapidly with the mass of the star. Consequently, we should not expect all the Cepheids to pulsate in the same mode and obey the same period–luminosity relation. It is not surprising that in Section 2 we found that the number distribution as a function of $\log(P)$ exhibits a two-component structure, separated at a period of around 10 days.

The differences in the pulsation characteristics between Cepheids with a range of periods are also borne out from the observed properties of Cepheids. The distribution of amplitude of light variation during a pulsation cycle against the period of pulsation shows some characteristics pointing to the mode of pulsation. From the GCVS (Kholopov et al. 1988), we plot the number density distribution of Galactic Cepheids against their V amplitudes for the two distinct period ranges (Figure 10). The number density at each value of V amplitude is computed by a moving average method in order to obtain smooth curves, and the distributions are normalized for direct comparison. The following features are evident from this comparative study. For Cepheids of period less than 10 days, the amplitude of oscillation in V -magnitude varies from less than 0.3 mag to upwards of 1.0 mag with an average of approximately 0.7 mag. More than 75% of these Cepheids have amplitude less than 0.85 mag. However, for period greater than 10 days, almost all the Galactic Cepheids in the catalogue have amplitudes greater than 0.7 mag, with an average of slightly over 1.0 mag. Only about 25% Cepheids in this period range have amplitudes less than 0.85 mag, and 35% of them have amplitudes higher than 1.1 mag. The catalogue of Caldwell and Coulson (1987) also indicates similar features in the distribution of V amplitudes over periods. Since it is known that the higher tone pulsators have less amplitude compared to those pulsating in the fundamental mode, such a distribution corroborates the hypothesis that lower period Cepheids are multi-mode pulsators as compared to fundamental mode pulsators which generally have higher periods.

Probably the shapes of light curves of the Cepheids are better indicators of the modes of pulsation. At periods between 8–16 days, there are multi-mode pulsators called bump Cepheids which are believed to oscillate in fundamental mode and the second harmonic. The bump is considered to be due to resonance between these two periods. At still lower periods, the beat Cepheids are considered to have period of the fundamental mode of radial oscillation slightly different from twice the pulsation period of the second harmonic causing the beat phenomenon. The MACHO project has revealed many beat Cepheids in LMC which pulsate at the fundamental mode and the first overtone, as well as the first and second overtones (Alcock et al. 1995).

Though there are other low period Cepheids which show smooth light curves, there are noticeable differences between the light and color curves of low and high period pulsators. In Figure 11 we have plotted the V light curves for a typical 7-day period Cepheid which shows a smooth variation of flux, and a 23-day period Cepheid for which the increase of luminosity with phase is faster and decrease much slower during the cycle. Also, the smaller period Cepheids often have a “shoulder” in the decreasing branch, which is not detected at higher periods (Figure 11). The observed minimum in the number of Galactic Cepheids as a function of their period is believed to be a consequence of mode switching around this

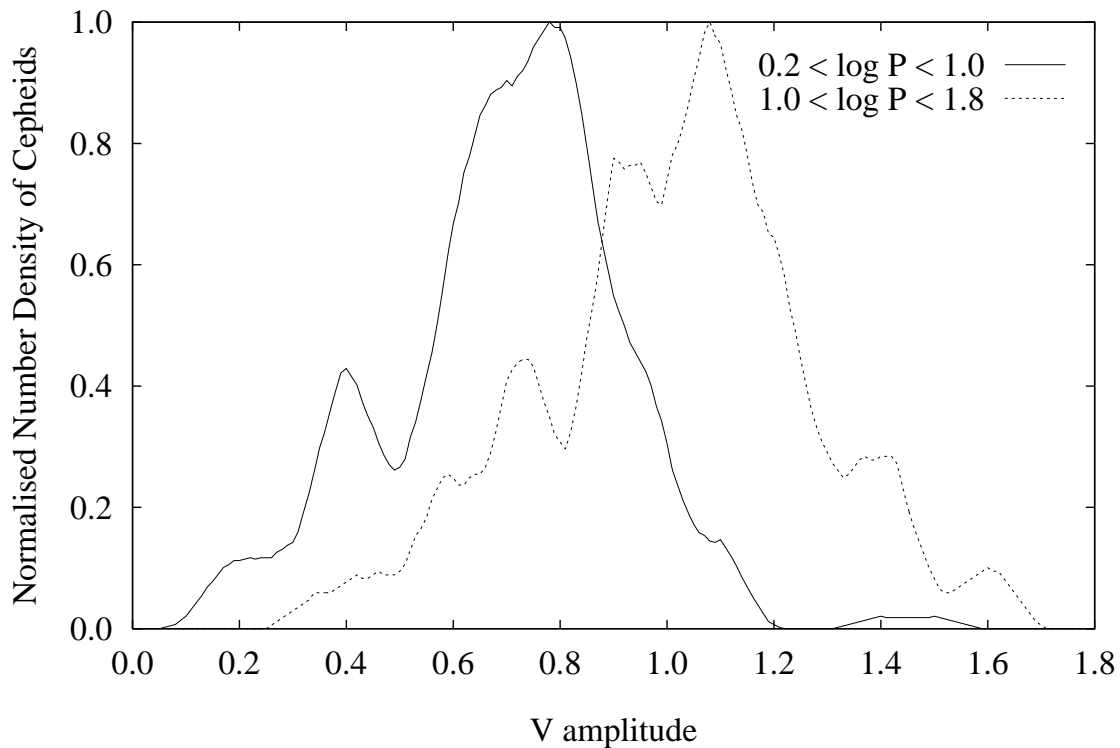


Fig. 10.— The normalized number density of Galactic Cepheids as a function of their V amplitudes of pulsation are shown for the two ranges of period: $0.2 < \log(P) < 1.0$ and $1.0 \leq \log(P) < 1.8$.

period, thereby producing a dip of approximately $\delta \log(P) \sim 0.15$ which represents the ratio between the periods of fundamental mode and the first harmonic. If, indeed, the Cepheids in the entire instability strip were to pulsate at various modes and their combinations, the Cepheid period–luminosity relation should have intrinsic scatter due to contributions from at least the following three sources:

1. The ratio of the period of fundamental mode to the second harmonic of approximately 2 will contribute a scatter of more than 0.3 mag in the V -magnitude.
2. The dynamical time and effective polytropic index are very different for Cepheids at the three different phases of evolution, though the consequent contribution to the period– V -magnitude relation is dependent on the details of stellar evolution. The scatter in the period–luminosity diagram due to structural changes during the three phases cannot therefore be quantified.
3. For a width of the instability strip of $\delta \log T_{\text{eff}} \sim 0.03$, the spread in the period at

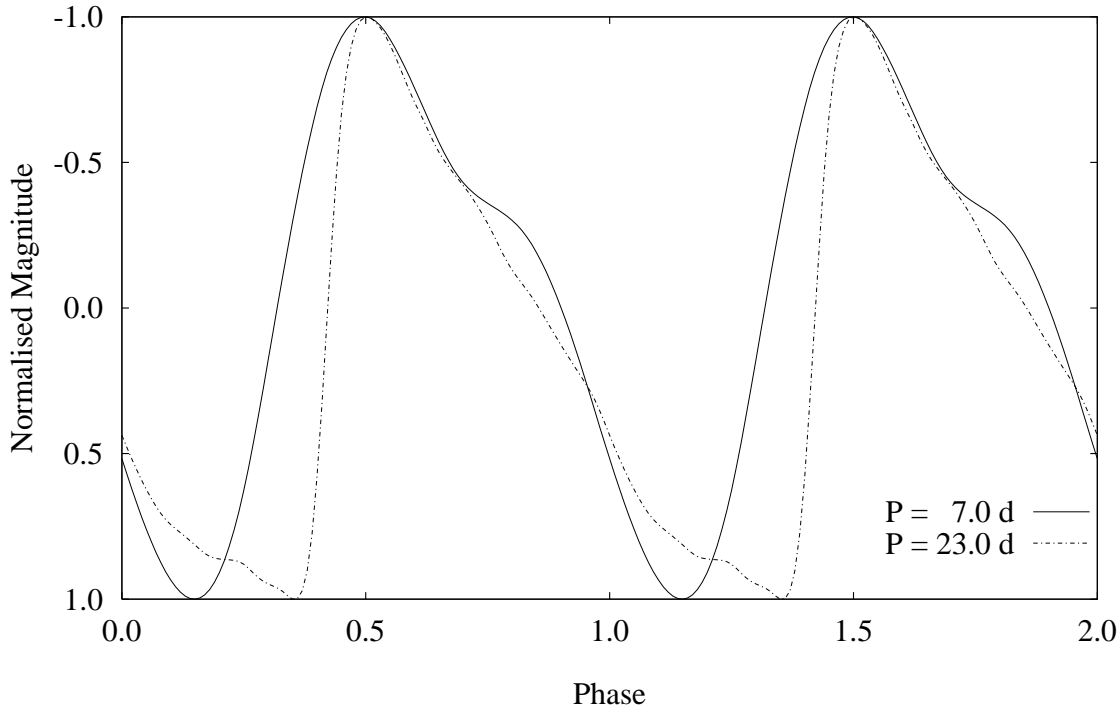


Fig. 11.— Typical light curves of Galactic Cepheids at periods 7^d (V1025 Cyg) and 23^d (WZ Car) are shown in a normalized form for comparison.

constant luminosity will be $\delta \log(P) \sim 0.09$ and consequent scatter in the V -magnitude vs period diagram could be ~ 0.3 mag.

4. Extraneous factors like metallicity, rotation and diffusion of elements contribute to the scatter in the period–luminosity relation but no concrete results are available yet.

The observed scatter in the period– V -magnitude relation does not appear to be substantially larger than 0.3 mag for the Cepheids of high period, in spite of additional errors due to extinction correction. Consequently, we are inclined to believe that most of the Cepheids of period larger than 15 days are likely to be fundamental mode pulsators. Ideally the problem should be sorted out by an explicit computation of the pulsation properties of the Cepheids and examination of the stability of the modes. However, Narasimha (1984) found that the stability of stars in this region of the HR diagram is crucially dependent on the treatment of the coupling between pulsation and convection. The following discussion is based on the results presented in his thesis.

When the surface temperature of a star is of the order of 8000 K, all the radial modes are stable, but the first harmonic is only marginally stable. The stability is a consequence of

the weakening of κ -mechanism in the helium ionization zone due to a decrease in the density (discussed in Section 7). At lower temperatures when the excitation due to κ -mechanism is stronger, the stability is governed by the onset of convection in the outer layers where bulk of the dissipation occurs. Many of the modes can be unstable, but at low enough value of the acceleration due to gravity at the photosphere, higher harmonics propagate into the atmosphere, because only the fundamental mode is trapped in the sub-atmospheric layers. This follows from the rate of variation of the acoustic cutoff frequency in the atmosphere with luminosity along the instability strip, where the temperature does not change appreciably but only mass and luminosity vary. The product (Γ) of the dynamical time scale of the star and the acoustic cutoff frequency varies as $\sqrt{\frac{GM}{RT_{\text{eff}}}}$, where \mathcal{M} is the stellar mass, R is the radius and T_{eff} is the effective temperature. The radius of the star increases by at least a factor of 5 between periods of 5 and 50 days while the mass of the Cepheid does not change by more than a factor of 3. Hence we should expect Γ to become less than 1.5 for a Cepheid of large period during its cool phase of pulsation. Consequently, only the fundamental mode can be trapped in the stellar envelope and the star can pulsate without energy leakage into the atmosphere. The higher modes should be traveling up in the atmosphere and dissipating energy at a rate governed by the local thermal time scale which is comparable to the pulsation period, and hence they cannot have well-defined periods. Consequently, irrespective of the the excitation mechanism for pulsation, the Cepheids of large enough period should be fundamental mode pulsators. The question is: where does the transition from fundamental mode to higher mode or a mixture of modes occur?

The dip in the number versus period of pulsation for the Galactic Cepheids, at around 10 day period, is indicative of the mode transition of the Cepheids. Most of the bump Cepheids occupy this transition region, between period of 9 to 18 days. In order to get a better picture, we appeal to the $\log T_{\text{eff}} - \log g$ plane for the Cepheids, where g is the acceleration due to gravity on the surface. Since the stellar atmospheric structure is determined from the value of g , T_{eff} and the chemical composition (subject to the uncertainties due to mechanical energy transport and dissipation in the atmosphere), we should, in principle, be able to use the observed colors of Cepheids to determine their g and T_{eff} . We have obtained the position of the Cepheids in the $\log T_{\text{eff}} - \log g$ plane by computing their extinction corrected $(U - B)_0$, $(B - V)_0$ and $(V - I)_0$ colors and have displayed those in Figure 5 (subject to the qualifications of Section 8). With the help of this figure, we have computed the acoustic cutoff frequency for an isothermal atmosphere and the corresponding time scale, \mathcal{P}_{ac} , given by,

$$\mathcal{P}_{\text{ac}} = 2\pi\sqrt{\frac{H_P}{g}}, \quad (11)$$

where H_P is the pressure scale height at the photosphere. In Figure 12 we have shown

\mathcal{P}_{ac} as a function of the period of the Cepheids. It is evident that, indeed, \mathcal{P}_{ac} tends to the pulsation period for Cepheids of period larger than 30 days, while at periods of around 15 days the fundamental mode as well as first and second harmonic are trapped below the atmosphere. This is consistent with the observed properties of bump Cepheids. Even for the simple isothermal model of the atmosphere of Cepheid variables of period substantially greater than 20 days, the first harmonic is likely to propagate into the atmosphere just after the star is hottest and is about to attain the maximum radius.

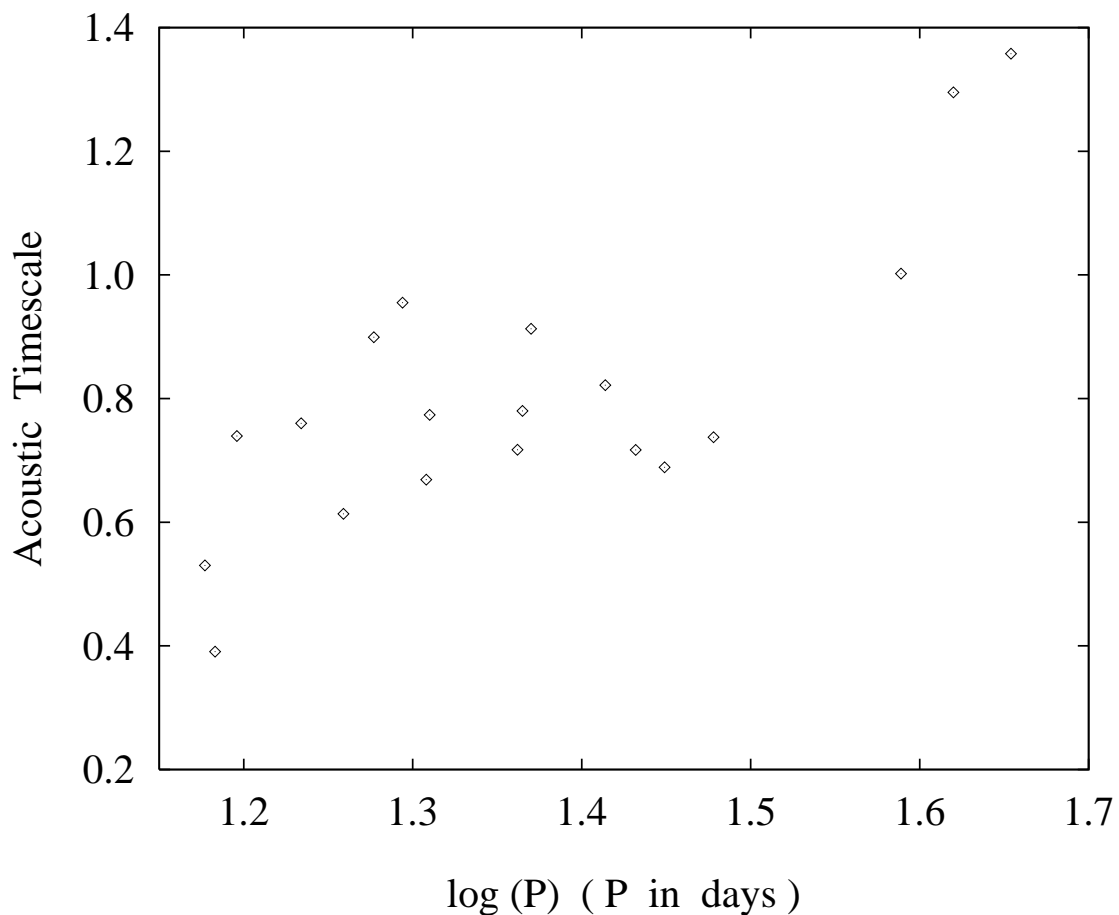


Fig. 12.— The acoustic time scale, \mathcal{P}_{ac} ($= 2\pi\sqrt{H_P/g}$), is plotted against $\log(P)$ for 19 Galactic Cepheids.

A word of caution is required: Cepheids are pulsators of large amplitude and their atmospheric structure undergoes substantial dynamical change during the pulsation cycle, apart from its being far from isothermal. Specifically, the convective overshoot into the

atmosphere introduces a large input of mechanical energy. Our discussion on the propagation of the waves into the atmosphere should therefore be treated as qualitative and indicative of the pulsation characteristics, rather than as a quantitative result. The individual points in the graph are not significant because the assumption that the 19 Cepheids are all fundamental mode pulsators is used for the computations.

With the help of Figure 1 on number density of classical Cepheids as a function of their periods, Figure 10 on the number distribution of Cepheids with respect to their amplitudes of pulsation at low and high periods, and Figure 12 relating to variation of the acoustic cutoff frequency with the period of pulsation, we are tempted to conclude that *Galactic Cepheids of pulsation period greater than 15 days should, in general, be considered to be fundamental mode pulsators*. Since this is the preferred population observed in distant galaxies, their pulsation properties should be studied independently of those of the low-period oscillators.

As we had discussed in Section 4, five of the stars were not considered in the final analysis because their statistically inferred positions in the $\log T_{\text{eff}} - \log g$ plane were far from the others. This could be attributed to errors in the U-band photometry, uncertainty in the computed value of extinction, or, these Cepheids might not be core helium burning stars. In the latter case, by determining the position of the star in the color diagram, we indeed have a method to identify the core helium burning Cepheids, which constitute the bulk of the stars in the instability strip.

6. Cepheid Masses

Once we trace the Cepheid instability strip in the $\log T_{\text{eff}} - \log g$ plane as a function of the period, we can in principle, use the period–luminosity relation to get an estimate of the mass of the Cepheid variables independent of the evolutionary or pulsation mass conventionally used. However, the method has two drawbacks, namely, (a) the strength of Balmer discontinuity and consequent change in $(U - B)$ for a supergiant of spectral type G depend on both the surface gravity and the hydrogen abundance in the envelope, and (b) the mapping from $(U - B)$ to g at fixed $(B - V)$ is susceptible to large magnifications in the errors in $(U - B)$ due to model atmospheric computations. Nevertheless, since the mass estimates of Cepheid variables could provide powerful constraints on the evolutionary models of stars of $7M_{\odot}$ to $20M_{\odot}$, we have tried to use our results to place the Cepheids in the evolutionary tracks adopted from Bressan et al. (1993).

We use the T_{eff} and g values as function of the period for the 19 Galactic Cepheid variables computed in Section 4 as well as the following period–luminosity relation adopted

from Paper II:

$$M_V = -3.45 \log(P) - 0.79 \quad (12)$$

The choice of the value of the slope of the period–luminosity relation is based on an analysis of Cepheids in several other galaxies and is discussed in detail in Paper II. The zero point is determined from Hipparcos measurement of trigonometric parallaxes of nearby Cepheids (Feast & Catchpole 1997). The luminosity at a given period is then computed, using the bolometric corrections given by Bessell et al. (1998).

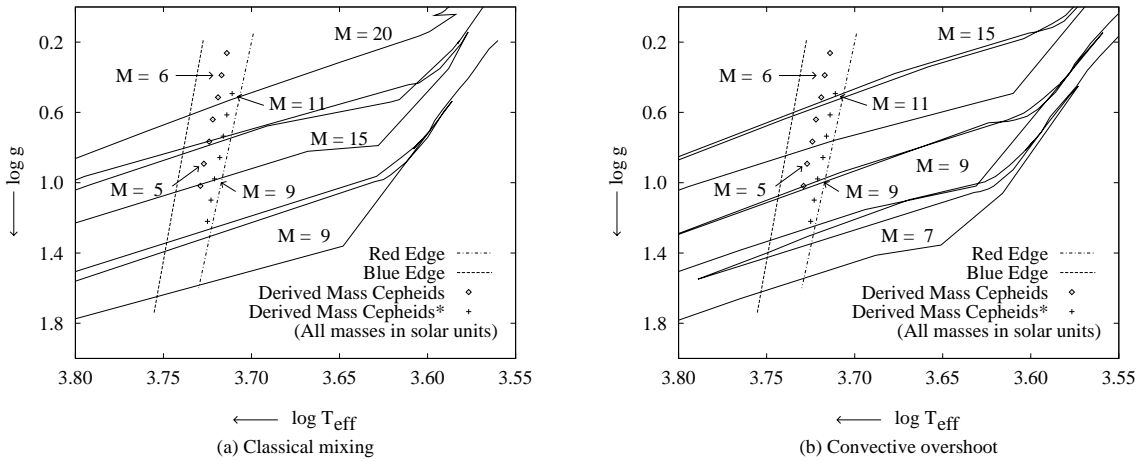


Fig. 13.— The evolutionary tracks of Bressan et al. (1993) have been plotted on the $\log T_{\text{eff}} - \log g$ plane, both for (a) classical mixing and (b) convective overshoot models. The expected mass of Cepheid variables between $1.2 \leq \log(P) \leq 1.8$ based on Figure 7 are shown. (* The mass estimates derived with the $(U - B)$ color for model atmosphere scaled by 1.02 are also shown with “+” symbols.)

We thus estimated the mass of the Cepheid variables along the instability strip and plotted them in the evolutionary track on a $\log T_{\text{eff}} - \log g$ plane in Figure 13. We compare our derived masses with those obtained from the evolutionary tracks of Bressan et al. (1993) for models with convective overshooting as well as without. Evidently, our masses are less by at least a factor 2 and the extraneous factors responsible to the discrepancy are discussed above. We can circumvent the problem by assuming that at the lower end of the period of the Cepheids (15 days), the evolutionary tracks should be consistent with our computed masses. This is easily achieved if we adopt the evolutionary tracks with convective overshooting and use the model atmospheric $(U - B)$ increased by less than 2%. As we had already demonstrated, this scaling affects the period–color–amplitude relations only in the third decimal. The estimated mass of around $8.2M_{\odot}$ for a period of 15 days is already slightly higher than the expected ZAMS mass of $8M_{\odot}$ for a star having same g value during its

second crossing of the instability strip. At higher periods, there is a progressively higher departure between the evolutionary mass and the one we have obtained. Consequently, even if we assume that for $\mathcal{M} \lesssim 9\mathcal{M}_\odot$, there is little mass loss up to core He burning, there should be substantial mass loss and other structural change modifying Q_0 for star of ZAMS mass $\sim 15\mathcal{M}_\odot$. Though too much emphasis should not be given to this discrepancy, we believe that the stars of higher mass ($\gtrsim 10\mathcal{M}_\odot$) should be losing considerable amount of mass during the red giant phase and that their effective polytropic index as measured from the quantity $(R/g)(2\pi/P)^2$ is different from that of low mass Cepheids.

7. Metallicity Dependency of the Instability Strip

Our work does not directly address the problem of metallicity effects on the Cepheid instability strip. Though ideally pulsation calculations should be carried out to address the problem, the coupling between pulsation and convection in the presence of supersonic convection in an extended envelope having very low density and relatively small thermal diffusion time does not provide any easy solution. However, in view of the extensive discussions occurring in the literature, we feel that the following remarks could be of some relevance:

It has been shown by various workers (cf. Becker, Iben & Tuggle 1977) that for a fixed temperature, the period–luminosity relation of a Cepheid variable does not appreciably depend on the chemical composition of the star (though as we pointed out at the beginning, indirectly there are certain small secondary effects). Consequently, the two major contributions to the correction to the period–luminosity relation due to difference in chemical composition will be due to

- (i) shift in the position of the instability strip in the HR diagram, and
- (ii) modifications to the stellar structure during the evolution.

Specifically, an increase in the temperature of the instability strip at constant luminosity by an amount of ΔT will produce a fractional decrease in the period of approximately $6\Delta T/T$. (Corrections due to stratification effects, though small, depend on the model of convection used). But the change in the stellar structure as well as evolutionary track crucially depends on the mass of the helium core just prior to helium burning. At present the change in the elemental abundance due to diffusion mechanism as well as convective overshooting are poorly understood and consequently, the detailed evolutionary calculations do not warrant a quantitative statement regarding its effect on the Cepheid instability strip.

We can get some insight into the position of the instability strip without any calculations involving specific models. The overstability of the radial modes in Cepheid variables is ascribed to the κ -mechanism. For envelopes of supergiants having large acceleration due to gravity ($\log g > 1.2$), the κ -mechanism operates in the H and He⁺ ionization zone at temperature in the range of 6000 to 13000 K as well as in a narrow He⁺⁺ ionization zone at temperature somewhere between 29000 K and 50000 K depending on the density of the layer and extent of the region having density inversion. If we assume that the H ionization zone determines the blue edge of the instability strip, beyond which energization due to κ -mechanism in the sub-photospheric layers undergoing hydrogen ionization is more than offset by the radiative damping in the deeper layers, the position of this boundary is insensitive to change in hydrogen abundance, *provided that, the metal abundance increases approximately as one sixth of the increase in helium abundance in the envelope.* For helium abundance of 0.3 by mass fraction the logarithm of temperature of the blue edge, $\log T_{\text{blue}}$ decreases by an amount of 0.005 for an increase in the metal abundance of 0.008 for fixed surface gravity. The blue edge determined in this form, using the opacity tables provided by Cox and Tabor (1976) as well as Cox (1991) is approximately along the line $\log T_{\text{eff}} = 3.759$, $\log g = 1.0$ and $\log T_{\text{eff}} = 3.787$, $\log g = 2.0$ for metal abundance $Z = 0.024$ and helium abundance $Y = 0.30$ by mass fraction when envelope models were run according to the prescriptions described in Narasimha (1984).

At low values of the surface gravity, hydrogen ionization zone alone does not determine the blue edge of the strip. But since the convective velocity is model-dependent and is a few tens of km s^{-1} , the structure of the envelope itself cannot be specified with any reliability unlike in the case of low luminosity stars. Still, if we use the strength of κ -mechanism both in the hydrogen and helium ionization zones as a measure of the pulsation instability, the position of the blue edge can be extended to surface gravity of the order of $\log g = 0.4$ from $\log g > 1$.

The blue edge determined in this form is in agreement with the extreme blue boundary obtained from the analysis of Galactic Cepheids (Section 4). Consequently, we are tempted to say that *the Cepheid instability strip is approximately 0.08 wide in $\log T_{\text{eff}}$ for fixed surface gravity and the position is weakly dependent on chemical composition if both helium and metal abundance in the zero age main sequence model are increased simultaneously.* However, it would be desirable to analyze colors of Cepheids of known chemical composition in the envelope using reliable atmospheric models to determine the sensitivity of the mean position of the instability strip as a function of chemical composition.

8. Main Limitations of the Work

In this work we have presented an analysis of observations relating to Cepheid variables compiled from various sources, coupled with theoretical considerations and simple calculations based on envelope models. Note the following limitations while using these results for calibrating the Cepheid instability strip:

1. The data we have used is culled from a number of sources. Note that the data have been compiled over more than thirty years, during which time the efficiency of detectors in U band has evolved and various workers may not have always taken into account the changes in the definition of different I band filters consistently. Though we have tried to cross-check the data and taken a sample which we consider to be trustworthy, it would be desirable to take a homogeneous sample from a single source for the kind of work we have carried out. Clearly, a systematic zero point error of 0.05 magnitude between data from two groups would lead to misleading final results. The size of our final sample—namely, 24 Cepheids having period greater than 15 days, 5 stars of which are at a different evolutionary phase—turns out to be small and could cause considerable random error in the relations we derived.
2. We adopted the model atmospheric data on the color vs T_{eff} and g from Bessell et al. (1998) after trying a few other available tables. However, they had to rescale their $(U - B)$ to match the observational data. We found that for the stars of our interest, namely, late F to early K supergiants, their original $(U - B)$ is better than the rescaled data and that by increasing the value by approximately 4%, we can get better agreement for the Cepheids. Fortunately, a change of 1% in their $(U - B)$ shifts the Cepheid instability strip by only 0.003 in $\log T_{\text{eff}}$ for a fixed g value and the slopes and intercepts of the period–color–amplitude relations change only in the third decimal, which is less than the typical errors in the slope. Nevertheless, it is clear that *if we calibrate a set of data on Cepheids using one model atmospheric scheme, we have to use the same scheme for another set of observations used to find the distance to a source or other characteristics of Cepheids.*

But we would like to stress that

- a. Our $\log T_{\text{eff}}$ at fixed period for the mean position of the instability strip could have an error of possibly more than 0.01 due to the above two limitations.
- b. The value of the mean g for a fixed period of the Cepheid is more sensitive to the errors caused by $(U - B)$. A change in the zero point of $(U - B)$ by 1% changes the derived mass by 30%. The fact that we have obtained a reasonable (though too low) mass for the Cepheids as well as extinction consistent with what is available in the literature indicates that probably our choice of Cepheid data as well as the model atmospheric

tables might not be bad.

3. We have not carried out any pulsation computations with full stellar models obtained from evolutionary sequence nor studied the effects of convection. Consequently, our statements on modes of pulsation of Cepheid variables having high period or the theoretical position of the instability strip should be treated as empirical.

4. We have been unable to get good enough sample of data for Cepheids in LMC or other galaxy where extinction is low and metallicity is very different from that of the Galaxy. To get an idea of the systematic errors in the calibration of the Cepheid period–luminosity relation, it is very desirable to carry out the required observations and analysis.

9. Conclusions

The principal outcome of the present work may be summarized as follows:

- * It appears that generally Galactic Cepheid variables of periods greater than 15 days are fundamental mode radial pulsators, while those with lower periods could be mixed mode pulsators or might even be oscillating at higher overtones.
- * A prescription to estimate the Cepheid $(V - I)$ light curve from the observed V light curve could be obtained based on the phase shift of $(V - I)|_{\text{at } V_{\text{min}}}$ with respect to the phase of V_{min} , whenever the data for the former is insufficient to draw an independent light curve.
- * Relations between pulsation period and color $((B - V), (V - I))$, as well as amplitude of light variation in V band and color at brightest phase, $(V - I)_0|_{\text{at } V_{\text{max}}}$ can be derived from the observed light curves. The extinction correction can be carried out either by using mean $(U - B)$, $(B - V)$ and $(V - I)$ as functions of period or from the mean $(V - I)$ and its value at the brightest phase of pulsation.
- * An estimation of Cepheid masses as function of period, is given by determining the instability strip in the $\log T_{\text{eff}} - \log g$ plane and using model atmospheres to argue that for stars with ZAMS mass greater than $10M_{\odot}$, mass loss and consequent structural changes cannot be neglected.
- * The metallicity effects on the Cepheid instability strip are estimated and the position of the blue edge of the strip is obtained from the strength of the κ -mechanism to find that the metallicity effect on the period–luminosity relation is not important if helium abundance increases with increasing metal abundance.

The limitations of the work should be noted while using our expressions and techniques for calibration of the Cepheid instability strip.

We are grateful to Fiorella Castelli for providing us the latest model atmospheres (ATLAS9) in an electronic format, and to S. M. Chitre for his critical comments on the manuscript. We acknowledge support from the Indo-French Center for the Promotion of Advanced Research (Project 1410-2).

REFERENCES

- Alcock, C., et al. 1995, *AJ*, 109, 1654
- Becker, S. A., Iben, I. Jr., & Tuggle, R. S. 1977, *ApJ*, 218, 633
- Berdnikov, L. N. 1992, *Astron. and Astrophys. Transactions*, 2, 43
- Berdnikov, L. N., & Turner, D. G. 1995, *Pis'ma Astr. Zhurnal*, 21, 803
- Bessell, M. S., Castelli, F., & Plez, B. 1998, *A&A*, in press
- Bressan, A., Fagotto, F., Bertelli, G., & Chiosi, C. 1993, *A&AS*, 100, 647
- Caldwell, J. A. R., & Coulson, I. M. 1987, *AJ*, 93, 1090
- Cardelli, J. A., Clayton, G. C., & Mathis, J. S. 1989, *ApJ*, 345, 245
- Coulson, I. M., & Caldwell, J. A. R. 1985, *SAAO Circulars*, 9, 5
- Coulson, I. M., Caldwell, J. A. R., & Gieren, W. P. 1985, *ApJS*, 57, 595
- Cox, A. N., & Tabor, J. E. 1976, *ApJS*, 31, 271
- Cox, A. N. 1991, private communication
- Chiosi, C., Wood, P. R., & Capitanio, N. 1993, *ApJS*, 86, 541
- Feast, M. W., & Catchpole, R. M. 1997, *MNRAS*, 286, L1
- Feast, M. W., & Walker, A. R. 1987, *ARA&A*, 25, 345
- Fernie, J. D., & Hube, J. O. 1968, *ApJ*, 73, 492
- Fernie, J. D. 1990, *ApJ*, 354, 295

- Fernie, J. D., Beattie, B., Evans, N. R., Seager, S. 1995, IBVS No. 4148
- Ferrarese, L., et al. 1996, ApJ, 464, 568
- Fouqué, P., & Gieren, W. P. 1993, A&A, 275, 213
- Freedman, W. L., & Madore, B. F. 1990, ApJ, 365, 186
- Gieren, W. P. 1989, A&A, 225, 381
- Iben, I. Jr., & Tuggle, R. S. 1975, ApJ, 197, 39
- Kennicutt, R., et al. 1998, ApJ, in press, (astro-ph/9712055)
- Kholopov, P. N., et al. 1988, General Catalogue of Variable Stars, 4th Ed., obtained from CDS, Strasbourg website (cdsweb.u-strasbg.fr)
- Labhardt, L., Sandage, A., & Tammann, G. A. 1997, A&A, 322, 751
- McMaster Cepheid Photometry and Radial Velocity Data Archive, website : www.physics.mcmaster.ca/Cepheid/HomePage.html
- Narasimha, D. 1984, Ph.D. thesis
- Silbermann, N. A., et al. 1996, ApJ, 470, 1